Applied Chemical Engineering (2026) Volume 9 Issue 1 ISSN: 2578-2010 (O)
doi: 10.59429/ace.v9i1.5812

ORIGINAL RESEARCH ARTICLE

Enhancing performance of planar structure single unit 800 °C O^{2-} SOFC at atmospheric pressure: A numerical modeling approach for electric power production

Ismail Benchebiba[1,*], Mohamed Mostefaoui[1], Ahmed Nour El Islam Ayad[2,3]

[1] *LGEER Laboratory, Faculty of Technology, Hassiba Benbouali University of Chlef, 02000, Algeria*

[2] *Electrical Engineering Department, Faculty of Applied Sciences, Kasdi Merbah University of Ouargla, 30000, Algeria*

[3] *APELEC Laboratory, Djilali Liabes University, Sidi Bel Abbes, 22000, Algeria*

***Corresponding author:** Ismail Benchebiba, i.benchebiba@univ-chlef.dz

ABSTRACT

Solid oxide fuel cells generate electricity with high electrical efficiency and flexibility in fuel use without emitting pollutants, such as carbon dioxide, nitrogen oxides, sulfur oxides and particulates. Nevertheless, they still face several obstacles and challenges that pose problems and questions driving researchers to find solutions. Numerical simulation is a key tool for integrating various physical fields, including charge dynamics, electrochemical pathways, chemical species kinetics, fluid flow, and energy transformations. The Butler-Volmer equation, in its various forms and approximations, is the most widely used equation for relating electrochemical pathways to current density in solid oxide fuel cell modeling. The main objective of this research is to model and simulate a high-temperature solid oxide fuel cell at atmospheric pressure, in order to test the effect of changing some properties values on the electrical power density produced. The results obtained revealed several techniques for enhancing the fuel cell performance, by improving the physical behaviors appropriate to each property on the corresponding side. It was found that fuel cell performance improves with increasing values of porosity rate, exchange current density, and pressure drop, and with decreasing both cell length and electrolyte thickness. Furthermore, since the electrolyte's conductivity class is oxygen ion carrier, the effect of parameters at the cathode side was more significant compared to the anode side. The results of this research are consistent with well-documented theories, and it is usable for developing other numerical models.

Keywords: solid oxide fuel cell; electrochemical; cathode; anode; electrical power

ARTICLE INFO

Received: 30 October 2025
Accepted: 17 December 2025
Available online: 27 January 2026

1. Introduction

Increasing electricity production with reducing polluting emissions is a pressing global necessity. Throughout history, diverse energy sources have been discovered, studied, and exploited, all contributing to meeting human needs. Suitable sources for producing electrical energy, such as the sun, wind, tides, and biomass, have proven their effectiveness[1]. Fuel cells have recently become a major focus of research; they are electrochemical technologies that can be classified according to operating temperature, fuel type, electrolyte material, and construction engineering[2,3]. The most commonly used fuel cell types are: Solid Oxide Fuel Cells (SOFCs), Polymer Electrolyte Fuel Cell or Proton Exchange Membrane Fuel Cells (PEMFCs), Phosphoric Acid Fuel Cells (PAFCs), Molten Carbonate Fuel Cells (MCFCs), Alkaline Fuel Cells (AFCs), and Direct Methanol Fuel Cells (DMFCs)[4]. Fuel cells are divided into two main categories

based on their operating temperature: low-temperature fuel cells and high-temperature fuel cells. Low-temperature fuel cells are suitable for transportation applications such as electric vehicles and include PEMFCs, PAFCs, DMFCs, and AFCs. High-temperature fuel cells are suitable for stationary power applications and include SOFCs and MCFCs[5,6]. SOFCs have high electrical efficiency up to 70%, high combined heat yield, long-term stability, fuel flexibility, low emissions, low maintenance costs, and a long theoretical life[7]. The solid electrolyte allows the cell to be manufactured in various self-supporting configurations, such as planar, monolithic, roll, and tubular[8-10]. However, the high operating temperature leads to long start-up times and mechanical and chemical compatibility problems[11]. The materials must possess unique and stringent properties due to the constraints and requirements imposed by the engineering of SOFCs, such as durability to prevent unwanted reactions and reliable thermal expansion[12]. The creation of SOFCs requires the development of chemically compatible materials with suitable conductivity, dimensional stability, strength, and high density[13]. Depending on the types of charge carriers in the electrolyte, two types are distinguished: oxygen-ion conducting (O^{2-}SOFC) and hydrogen-ion conducting (H^{+}SOFC)[14].

Numerical simulation is a very useful tool for understanding the various mechanisms and phenomena related to the behavior of fuel cells from several aspects. For example, Wei Kong et al. studied the effect of anode and cathode rib widths on gas diffusion and cathode-supported SOFC performance. They found that SOFC performance is strongly affected by rib width and that the optimal anode rib width is smaller than the optimal cathode rib width[15]. Jee Min Park et al. investigated how electrolyte thicknesses ranging from 80 to 100 µm and operating temperatures ranging from 700 to 800 °C affect electrochemical reactions and thermo-fluidic characteristics within a planar SOFC unit. They found that the maximum electrical power density increases with decreasing electrolyte thickness and that cell performance improves with increasing operating temperature[16]. Xuan-Vien Nguyen investigated how operating conditions, fuel concentration, and electrode porosity affect the electrochemical performance of electrodes. The results showed that improving fuel mass transfer requires higher electrode porosity and that increasing the operating temperature improves electrical potential distribution across electrode surfaces[17].

This article focuses on testing the effect of certain structural and electrochemical properties on the change in electrical power produced by a single-unit fuel cell. In section 2, the computational model of O^{2-}SOFC is described, including the operating process of O^{2-}SOFC, computational settings, and governing equations. In section 3, the simulation results are presented. In section 4, a conclusion highlighting the findings of this work is available.

2. Computational Model of O^{2-}SOFC

2.1. Operating mechanism of O^{2-}SOFC

In O^{2-}SOFCs, humidified air flows through the cathode channel while humidified hydrogen flows through the anode channel. The movement of electrons from the anode to the cathode generates electrical energy via an external circuit, as illustrated in **Figure 1**.

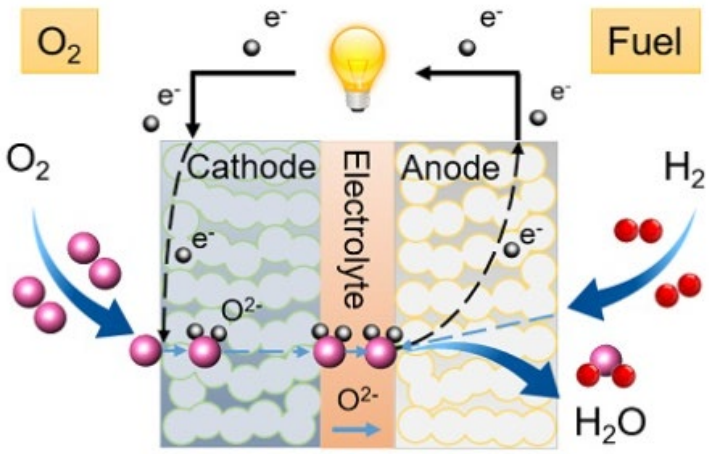

Figure 1. Operating principle of O^{2-}SOFC[18].

The two half reactions at both electrodes, and the full reaction are listed in **Table 1**.

Table 1. Electrochemical reactions in O^{2-}SOFC.

Side	Chemical/Electrochemical Reactions
Cathode	$1/2O_2 + 2e^- \rightarrow O^{2-}$
Anode	$H_2 + O^{2-} \rightarrow H_2O + 2e^-$
Overall	$1/2O_2 + H_2 \rightarrow$ Electric Power + Heat + H_2O

2.2. Planar-structure single-unit of O^{2-}SOFC

The planar-structure single-unit of O^{2-}SOFC model comprises two gas flow channels, two porous gas diffusion electrodes, and a single electrolyte. **Figure 2** shows the YZ plan, and **Figures 3** shows the XY and XZ plans.

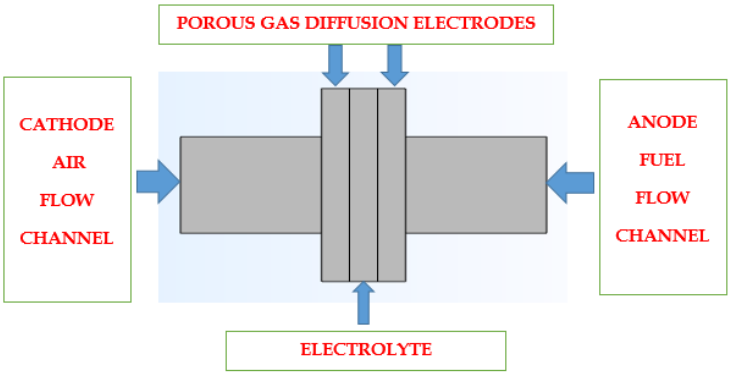

Figure 2. YZ-Plan Design for Planar-Structure Single-Unit O^{2-}SOFC Model.

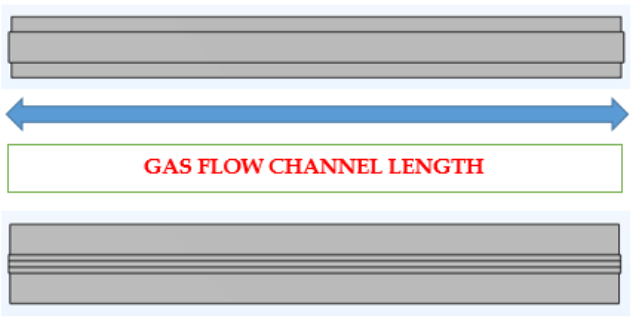

Figure 3. XY and XZ Plans Design for Planar-Structure Single-Unit O^{2-}SOFC Model.

Table 2 lists the initial structural properties of the O^{2-}SOFC model.

Table 2. Initial Structural Settings of O^{2-}SOFC Computational Model[19].

Structural Settings	Value and Unit
Gas Flow Channel Width	0.5 mm
Rib Width	0.5 mm
Porous Gas Diffusion Electrode Thickness	0.1 mm
Electrolyte Thickness	0.1 mm
Gas Flow Channel Height	0.5 mm
Cell Length	10 mm

2.3. Boundary conditions

The boundary conditions at the cathode and anode inflow are listed in **Table 3**.

Table 3. Boundary Conditions of O^{2-}SOFC Computational Model.

Boundary Conditions	Cathode-Side Inflow	Anode-Side Inflow
Electric Potential	1 V	0 V
Species Mass Fraction	O_2 : N_2 : H_2O = 0.15 : 0.48 : 0.37	H_2 : H_2O = 0.4 : 0.6
Pressure Drop	6 Pa	2 Pa

2.4. Kinetic species settings

Table 4 and **Table 5** list the properties relating to the diffusivity of the fuel and air species, including effective diffusivity, kinetic volume, molar mass, reference diffusivity, and binary diffusivity.

Table 4. Kinetic Species Characteristics[20,21].

Species	Effective Diffusivity	Kinetic Volume	Molar Mass
O_2	1.2018×10^{-5} m^2/s	16.3×10^{-6} m^3/mol	0.032 kg/mol
N_2	1.2342×10^{-5} m^2/s	18.5×10^{-6} m^3/mol	0.028 kg/mol
H_2	4.9825×10^{-5} m^2/s	6.12×10^{-6} m^3/mol	0.002 kg/mol
H_2O	2.7041×10^{-5} m^2/s	13.1×10^{-6} m^3/mol	0.018 kg/mol

Table 5. Binary Diffusivity Data of O^{2-}SOFC Computational Model[20,21].

Diffusion Parameters	Value and Unit
Reference diffusivity	3.16×10^{-8} m^2/s
Binary diffusivity of O_2 and N_2	1.9235×10^{-4} m^2/s
Binary diffusivity of H_2 and H_2O	8.1794×10^{-4} m^2/s
Binary diffusivity of O_2 and H_2O	3.2674×10^{-5} m^2/s
Binary diffusivity of N_2 and H_2O	2.4477×10^{-4} m^2/s

2.5. Electrochemical properties of SOFC model

The electrochemical settings are listed in **Table 6**.

Table 6. Electrochemical Settings of O^{2-}SOFC Computational Model[22-26].

Electrochemical properties	Cathode-Side	Anode-Side	Electrolyte-Side
Exchange Current Density	0.01 A/m^2	0.1 A/m^2	-

Electrochemical properties	Cathode-Side	Anode-Side	Electrolyte-Side
Equilibrium Voltage	1 V	0 V	-
Permeability	10^{-10} m^2	10^{-10} m^2	-
Porosity Rate	40%	40%	-
Viscosity	Air : 4.4574×10^{-5} Pa.s	H_2 : 2.4320×10^{-5} Pa.s	-
Specific Surface Area	10^9 m^{-1}	10^9 m^{-1}	-
Electrolyte Effective Conductivity	1 S.m^{-1}	1 S.m^{-1}	-
Solid Effective Conductivity	1000 S.m^{-1}	1000 S.m^{-1}	-
Electrolyte Conductivity	-	-	5 S.m^{-1}

Table 6. (*Continued*)

2.6. Related equations

To activate various mechanisms and balance the behavior of phenomena, certain processes must be included in fuel cell modeling. Solid oxide fuel cell modeling is primarily based on electronic and ionic charge balances, charge transfer kinetics, mass balances, and flow distribution.

The current densities in the electrolyte i_l and solid electrode i_s , as well as the electron Q_s and ion Q_l current densities, are given by OHM's law with charge balance[27]:

$$i_l = -\sigma_l \nabla \emptyset_l \quad (1)$$

$$i_s = -\sigma_s \nabla \emptyset_s \quad (2)$$

$$Q_s = \nabla \cdot i_s \quad (3)$$

$$Q_l = \nabla \cdot i_l \quad (4)$$

Here σ_l and σ_s are the ionic and solid electrode conductivities, respectively, and $\emptyset_l$ and $\emptyset_s$ are the electrolyte ionic and solid electrode potentials, respectively.

Several expressions of the BUTLER-VOLMER equation are considered depending on the cases of electrochemical electrode kinetics cases[28]. The concentration-controlled BUTLER-VOLMER equation governs the charge transfer current density at the anode i_{act} and the cathode i_{cct} :

$$i_{act} = i_{0a}\left[\frac{c_{H_2}}{c_{H_2}^{ref}}\exp\left(\frac{0.5F}{RT}\eta\right) - \frac{c_{H_2O}}{c_{H_2O}^{ref}}\exp\left(\frac{-1.5F}{RT}\eta\right)\right] \quad (5)$$

$$i_{cct} = i_{0c}\left[\exp\left(\frac{3.5F}{RT}\eta\right) - x_{O_2}\frac{c_t}{c_{O_2}^{ref}}\exp\left(\frac{-0.5F}{RT}\eta\right)\right] \quad (6)$$

Where i_{0a} : Initial anode-side exchange current density, c_{H_2} : Hydrogen concentration, c_{H_2O} : Water concentration, $c_{H_2}^{ref}$: Hydrogen reference concentration, $c_{H_2O}^{ref}$: Water reference concentration, R: Gas constant, F: Faraday's constant, T: Operating temperature, η: Activation over-potential, i_{0c} : Initial cathode-side exchange current density, $c_{O_2}^{ref}$: Oxygen reference concentration, x_{O_2} : Oxygen fraction, c_t : Total concentration.

The activation over-potential is related to the equilibrium electrode potential E_{eq}, as follows:

$$\eta = \emptyset_s - \emptyset_l - E_{eq} \quad (7)$$

The expression of cell voltage V_{cell} depends on the cell polarization V_{pol}, as shown below:

$$V_{cell} = \varphi_c - \varphi_a - V_{pol} \quad (8)$$

Where φ_c and φ_a are the electric potential at the cathode-side inlet and anode-side inlet, respectively.

3. Results and discussion

3.1. Voltage-current-power curves

The cell current density is low when the cell voltage is high and high when the cell voltage is low[29]. The change in cell current density I_{cell} as a function of the input cell voltage range can be expressed as follows:

$$I_{cell} = f(V_{cell}) \tag{9}$$

The produced cell power density P_{cell} is calculated, as follows:

$$P_{cell} = V_{cell} \times I_{cell} \tag{10}$$

Under the same operating conditions, the cell voltage is inversely proportional to the cell current density. On the other hand, the cell power density initially increases to reach a peak value of 1132 W/m², and then decreases as the cell current density increases, as illustrated in **Figure 4**. These results are consistent with the available literature[30].

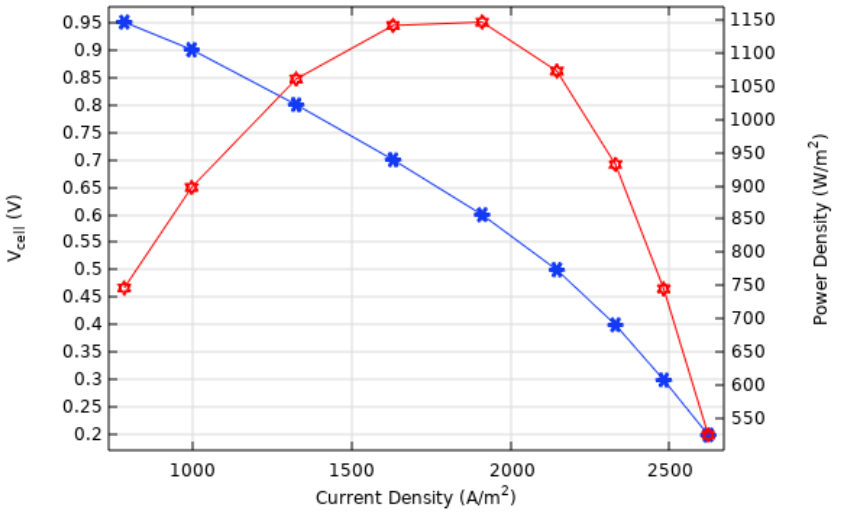

Figure 4. V-I-P Curves for Initial Operating Conditions.

3.2. Effect of porous gas diffusion electrodes porosity

The porosity is defined as the percentage of a material's volume occupied by pores or voids[31]. It is expressed as a fraction or percentage, given by the following formula:

$$P(\%) = \frac{V_p}{V_b} \times 100 \tag{11}$$

Here P is the porosity rate, V_p is the total pores volume per unit volume, V_b is the bulk volume of the porous materials per unit volume.

In materials physics, an increase in porosity rate refers to an increase in the size or number of pores embedded in the porous material. This improves the diffusion rate of chemical species through porous gas diffusion electrodes (PGDEs) in solid oxide fuel cells. Taking into account the independence of the porosity rate from any other physical or fluid property and maintaining the same initial operating conditions. This approach opens the possibility of increasing the porosity rate directly as a percentage as illustrated in **Figure 5** where the peak power density reaches 1146 W/m² at 55% or by increasing the thickness of PGDEs as illustrated in **Figure 6** where the peak power density reaches 1250.8 W/m² for 160 µm PGDEs thickness. This defines a direct proportionality that can be expressed as follows:

$$P^{new}(\%) = \frac{P^{old}(\%) \times V_b^{new}}{V_b^{old}} \tag{12}$$

Here P^{new} is the new porosity rate after changing (increasing or decreasing) the bulk volume of the porous material, P^{old} is the initial porosity rate before changing the bulk volume of the porous material. V_b^{new} and V_b^{old} are the new bulk volume and the initial bulk volume of the porous material, respectively.

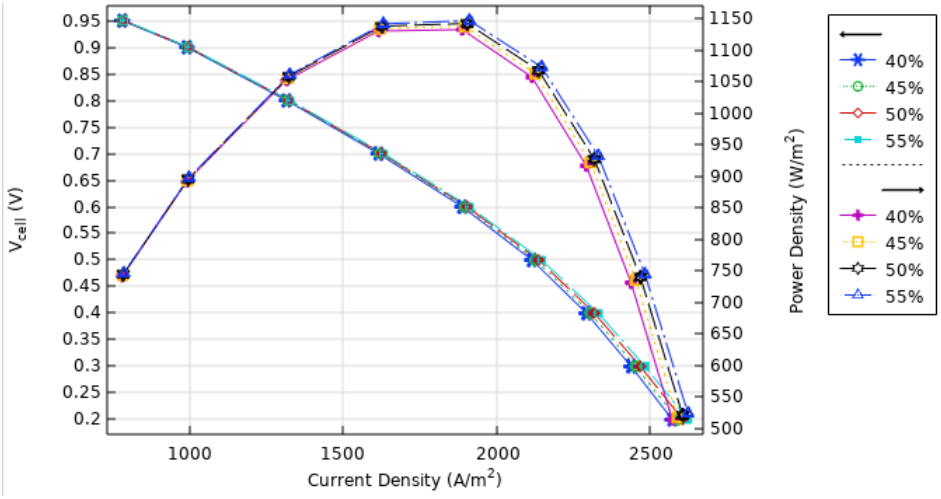

Figure 5. Effect of PGDEs Porosity Percentage on V-I-P Curves.

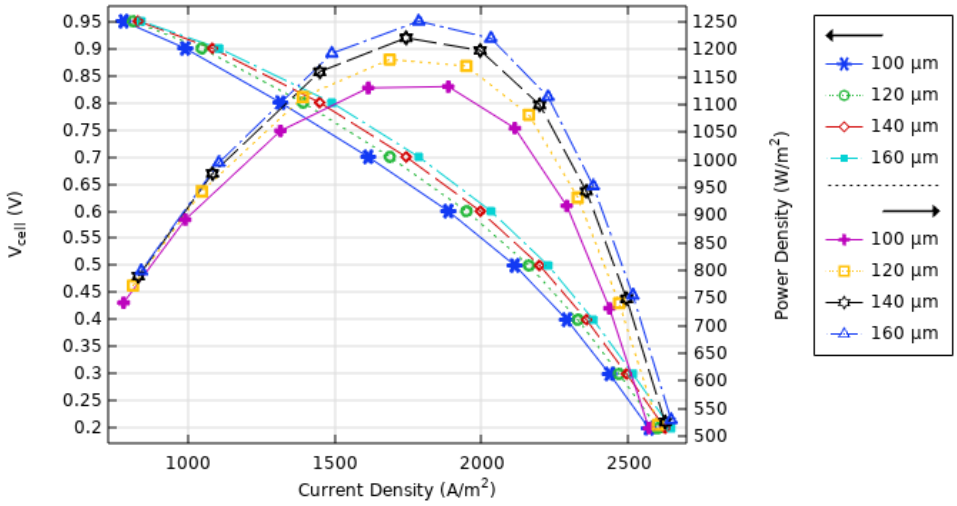

Figure 6. Effect of PGDEs Thickness on V-I-P Curves.

3.3. Effect of exchange current density

The reaction rate coefficient in chemistry is analogous to the exchange current density in electrochemistry[32], meaning that chemical reactions with a high reaction rate coefficient are more significant than those with a lower reaction rate coefficient, some of which are neglected in certain studies. Similarly, the higher the exchange current density, the better the performance of the electrochemical fuel cell, and vice versa. Numerous examples in the literature demonstrate the direct relationship between increasing exchange current density and the efficiency of electrochemical systems. For example, Raj Kamal Abdul Rashid et al. reported that exchange current density is a good measure of catalyst reaction rate, and that a higher value indicates better electrochemical performance of a pulsed electrochemical fuel cell[33]. Harshad Bandal et al. suggest that exchange current density reflects the intrinsic interconnection and charge-transfer interactions of electro-catalysts. In other words, high exchange current densities generally indicate excellent catalytic activity[34]. The

results obtained are in satisfactory agreement with the outcomes of the aforementioned examples, where the peak power density reaches 1550 W/m² for 0.04 A/m² cathode-side exchange current density as shown in **Figure 7** and 1172 W/m² for 0.4 A/m² anode-side exchange current density as shown in **Figure 8**.

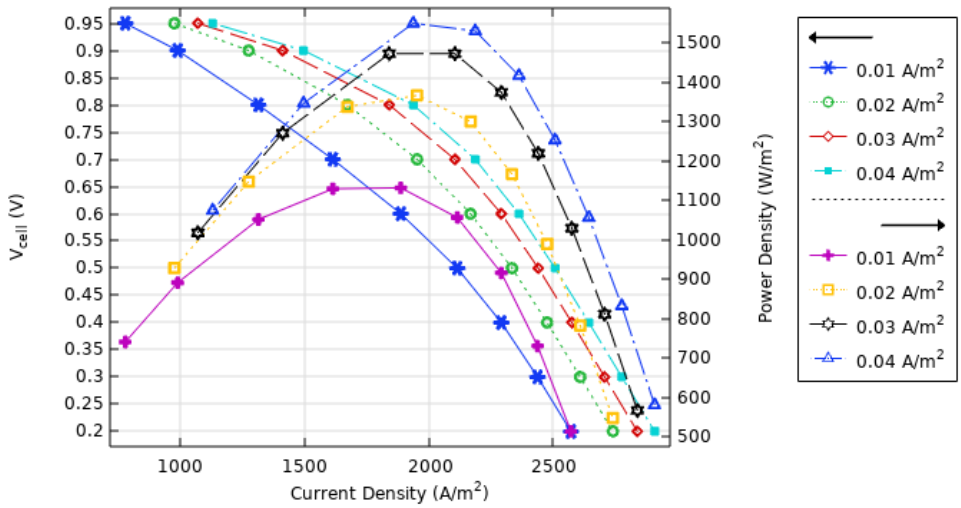

Figure 7. Effect of Cathode-Side Exchange Current Density on V-I-P Curves.

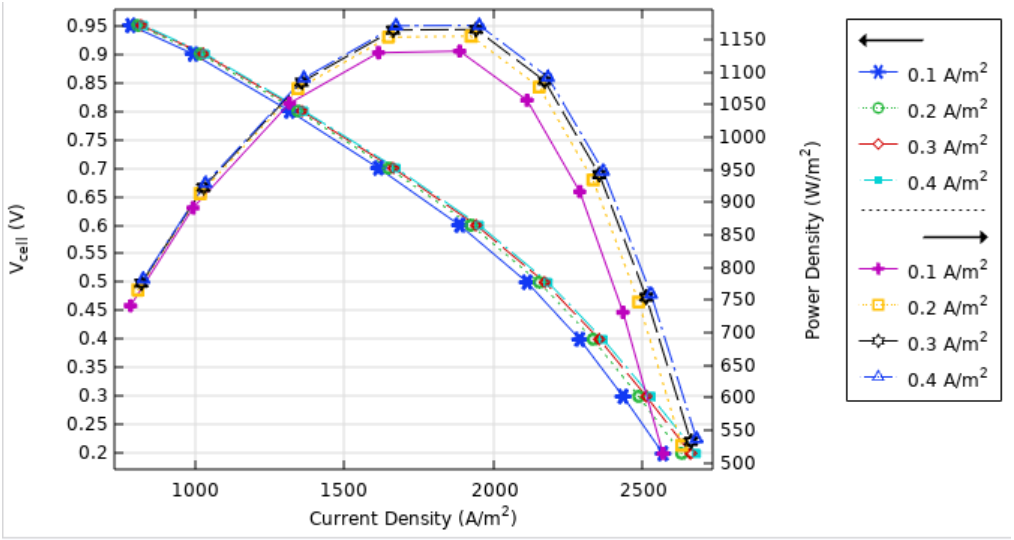

Figure 8. Effect of Anode-Side Exchange Current Density on VI-P Curves.

3.4. Effect of pressure drops

A pressure drop occurs when a gas experiences a decrease in pressure as it flows through a channel. This results in a pressure difference between the gas inflow and gas outflow[35]. When gas (such as air or fuel) flows, a frictional forces are created due to the channel's resistance, which drops the gas pressure. The resistance to gas flow through channels depends on the dynamic and fluid properties of the gases, such as viscosity and velocity. The greater the gas flow rate, the greater the pressure drop at the related electrode (anode for fuel and cathode for air). Therefore, if the gas is highly flowing, the pressure drop will also be higher, and vice versa. The peak power density reaches the values of 1316 W/m² for 9 Pa at the cathode-side and 1142 W/m² for 5 Pa at the anode-side, as illustrated in **Figure 9** and **Figure 10** respectively. Another solution to make the pressure drop effect more pronounced is to increase the resistance of the gas flow channels by decreasing the cell length. **Figure 11** shows that as the cell length decreases, the peak power density increases, reaching 1515 W/m² at a cell length of 7 mm.

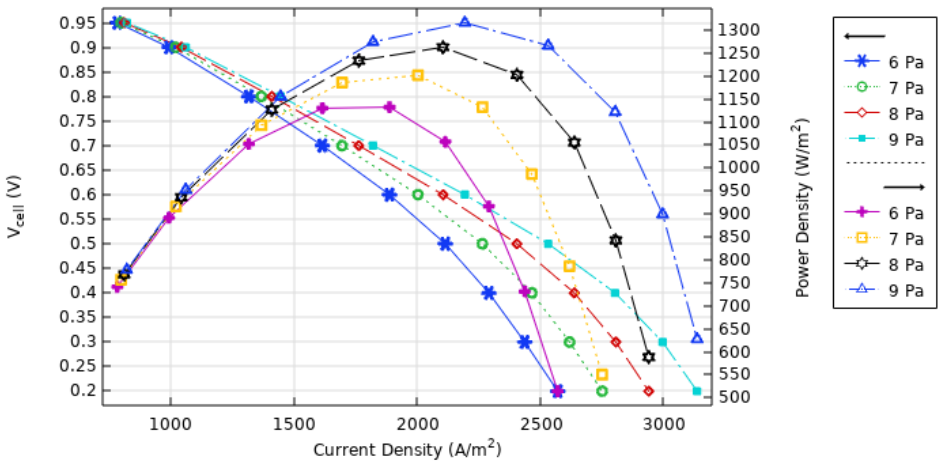

Figure 9. Effect of Cathode-Side Pressure Drop on V-I-P Curves.

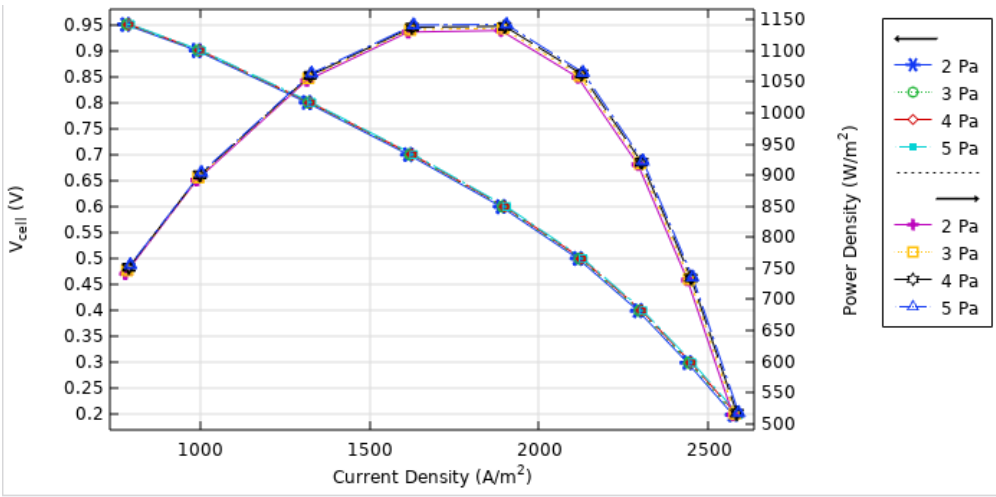

Figure 10. Effect of Anode-Side Pressure Drop on V-I-P Curves.

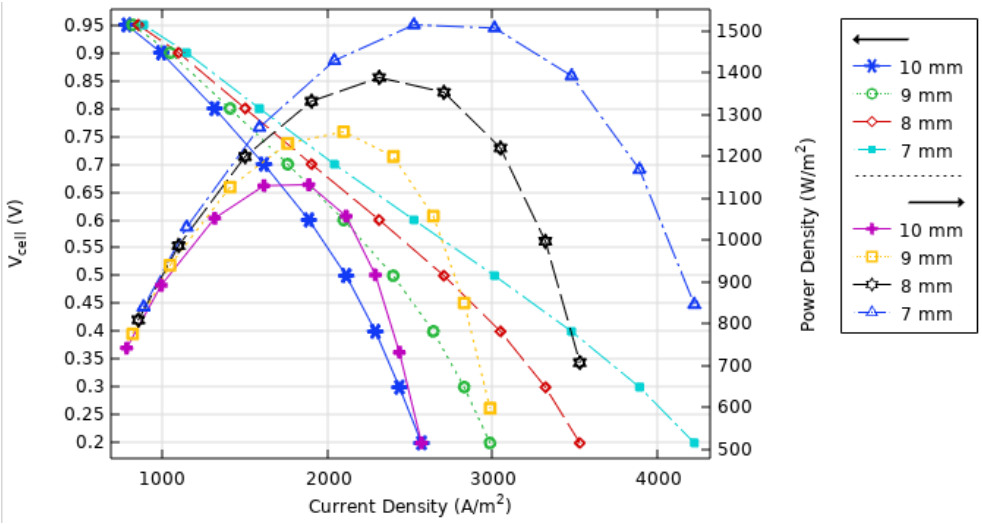

Figure 11. Effect of Single-Unit Cell Length on V-I-P Curves.

3.5. Effect of gas flow channel dimensions

Increasing the height or width of the gas flow channels increases their gas capacity, which improves the amount of gas flowing through them in terms of mass transfer, distribution, diffusion, and flow. Consequently,

the fuel cell performs more efficiently. As the height of the gas channels increases, the fluid and physical properties of the gases inside the channels improve vertically. And as the width of gas channels increases, the fluid and physical properties of the gases across the channels improve horizontally. The peak power density reached a values of 1525 W/m² and 1416 W/m² for 0.8 mm height and 0.8 mm width , as illustrated in **Figure 12** and **Figure 13**, respectively.

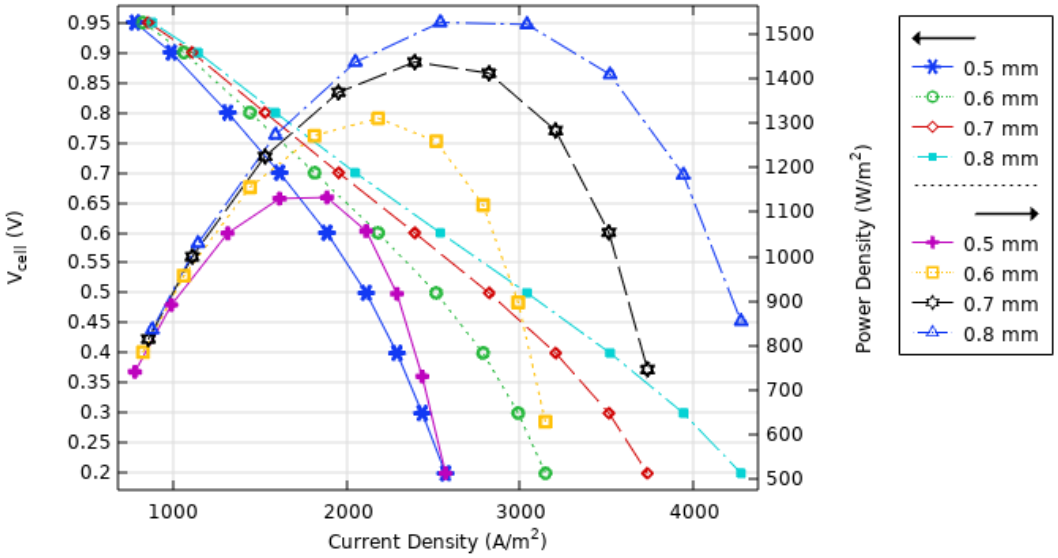

Figure 12. Effect of Gas Flow Channel Height on V-I-P Curves.

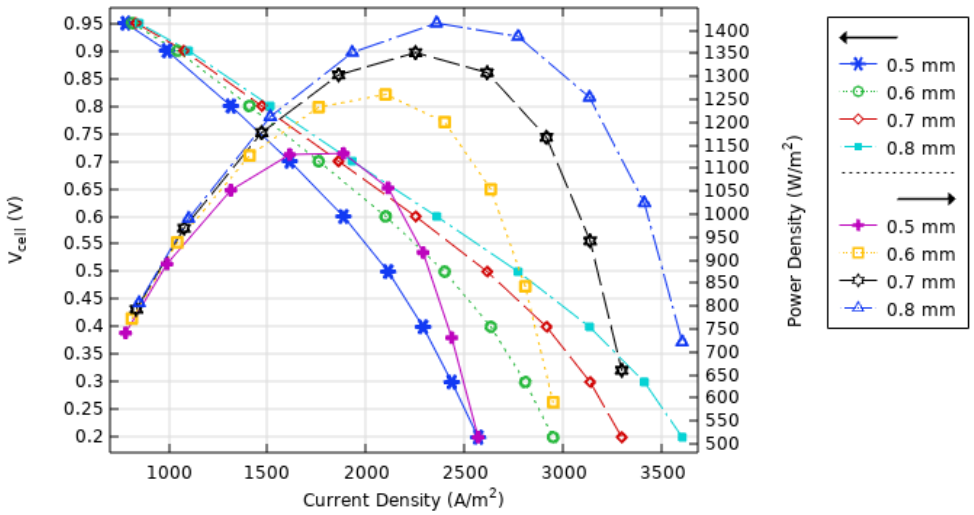

Figure 13. Effect of Gas Flow Channel Width on V-I-P Curves.

3.6. Effect of electrolyte thickness

The electrolyte is the core of a fuel cell, acting as an ionic conductor between the electrodes. The thickness of the electrolyte plays a key role in the overall performance of the cell. Reducing the electrolyte thickness results in better ionic conductivity and less heat loss. As reported by Jee Min Park et al[16], the thinner the electrolyte, the better the solid oxide fuel cell performs. The peak power density reaches 1190 W/m² for electrolyte thicknesses of 10 µm as shown in **Figure 14**.

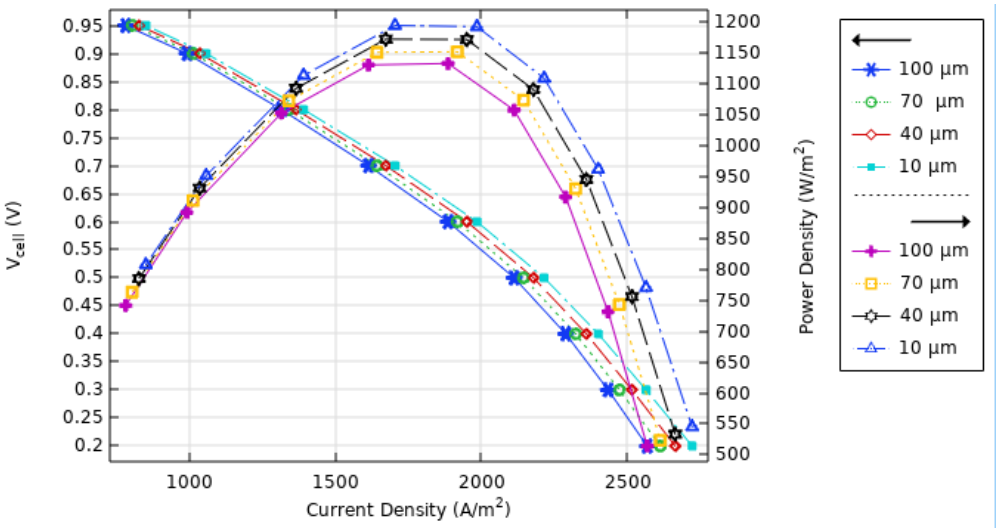

Figure 14. Effect of Electrolyte Thickness on V-I-P Curves.

Table 7 summarizes the key elements related to improving cell performance and linking them to the corresponding component.

Table 7. Summary linking appropriate physical switches to the fuel cell component.

O^{2-}SOFC Component	Physical properties	Related physical behaviors
Electrodes	Porosity rate	Species diffusion rate
Electrodes	Exchange current density	Charge transfer
Gas flow channels	Pressure drops	Frictional forces Channel's resistance Gas flow rate Gas viscosity and/or velocity
Gas flow channels	Dimensions (Height and Width)	Species mass transfer, propagation, distribution, and flow rates
Electrolyte	Thickness	Ionic conductivity

4. Conclusion

In conclusion, fuel cells are a leading technology in the field of renewable energy, and aim to produce electrical power to operate external circuits. This paper has presented a numerical simulation of a high-temperature solid oxide fuel cell for finding the best ways to improve fuel cell performance. The theoretical model was based on Ohm's law with charge balance, the Butler-Volmer equation, and activation over-potential. The findings revealed several methods to improve oxygen mass transport, ultimately optimizing the output electric power density. Overall, to improve the yield of a O^{2-}SOFC, strategies can be summarized through:

- Bettering the ionic conductivity through reducing the electrolyte thickness.
- Enhancing the physics behaviors of the chemical species.
- Optimizing the structure dimensions.

Conflict of interest

The authors declare no conflict of interest.

References

1. Wilk-Jakubowski J L, Pawlik L, Wilk-Jakubowski G, et al. State-of-the-Art in the Use of Renewable Energy Sources on the Example of Wind, Wave Energy, Tidal Energy, and Energy Harvesting: A Review from 2015 to 2024. Energies. 2025. 18: 1356. https://doi.org/10.3390/en18061356
2. Sazali N, Wan Salleh WN, Jamaludin AS, et al. New Perspectives on Fuel Cell Technology: A Brief Review. Membranes. 2020. 10: 99. https://doi.org/10.3390/membranes10050099
3. Jawad NH, Yahya AA, Al-Shathr AR, et al. Fuel Cell Types, Properties of Membrane, and Operating Conditions: A Review. Sustainability. 2022: 14; 14653. https://doi.org/10.3390/su142114653
   Lo Vecchio C, Sebastián D, Lázaro MJ, et al. Methanol-Tolerant M–N–C Catalysts for Oxygen Reduction Reactions in Acidic Media and Their Application in Direct Methanol Fuel Cells. Catalysts 2018: 8: 650. https://doi.org/10.3390/catal8120650
4. Fakhreddine O, Gharbia Y, Derakhshandeh JF, et al. Challenges and Solutions of Hydrogen Fuel Cells in Transportation Systems: A Review and Prospects. World Electric Vehicle Journal. 2023, 14, 156. https://doi.org/10.3390/wevj14060156
5. Elkafas A G, Rivarolo M, Gadducci E, et al. Fuel Cell Systems for Maritime: A Review of Research Development, Commercial Products, Applications, and Perspectives. Processes. 2023: 11: 97. https://doi.org/10.3390/pr11010097
6. Helal H, Ahrouch M, Rabehi A, et al. Nanostructured Materials for Enhanced Performance of Solid Oxide Fuel Cells: A Comprehensive Review. Crystals; 2024, 14, 306. https://doi.org/10.3390/cryst14040306
7. Pianko-Oprych P, Zinko T, Jaworski Z. A Numerical Investigation of the Thermal Stresses of a Planar Solid Oxide Fuel Cell. Materials. 2016, 9, 814. https://doi.org/10.3390/ma9100814
8. Hodjati-Pugh O, Dhir A, Steinberger-Wilckens R. The Development of Current Collection in Micro-Tubular Solid Oxide Fuel Cells—A Review. Appl. Sci. 2021, 11, 1077. https://doi.org/10.3390/app11031077
9. Mendonça C, Ferreira A, Santos DMF. Towards the Commercialization of Solid Oxide Fuel Cells: Recent Advances in Materials and Integration Strategies. Fuels: 2021, 2, 393-419. https://doi.org/10.3390/fuels2040023
10. Yahyazadeh A. A Comprehensive Review of the Development of Perovskite Oxide Anodes for Fossil Fuel-Based Solid Oxide Fuel Cells(SOFCs):Prospects and Challenges. Physchem. 2025, 5, 25. https://doi.org/10.3390/physchem5030025
11. Sun R, Li S, Gao L, et al. Ni-Doped Pr0.5Ba0.5CoO3+δ Perovskite with Low Polarization Resistance and Thermal Expansivity as a Cathode Material for Solid Oxide Fuel Cells. Molecules. 2025, 30, 1482. https://doi.org/10.3390/molecules30071482
12. Patel VK, Gholamalian F, Kalyvas C, et al. Modelling Mass Transport in Anode-Supported Solid Oxide Fuel Cells. Electronics 2025; 14; 3486. https://doi.org/10.3390/electronics14173486
13. Kuterbekov KA, Nikonov AV, Bekmyrza KZ, et al. Classification of Solid Oxide Fuel Cells. Nanomaterials 2022, 12, 1059. https://doi.org/10.3390/nano12071059
14. Kong W, Gao X, Liu S, et al. Optimization of the Interconnect Ribs for a Cathode-Supported Solid Oxide Fuel Cell. Energies 2014, 7, 295-313. https://doi.org/10.3390/en7010295
15. Park JM, Kim DY, Baek JD, et al. Effect of Electrolyte Thickness on Electrochemical Reactions and Thermo-Fluidic Characteristics inside a SOFC Unit Cell. Energies 2018, 11, 473. https://doi.org/10.3390/en1103047
16. Nguyen XV, Three-Dimensional Simulation of the Operating Characteristics of Cell Layers in Solid Oxide Fuel Cells. Appl. Sci. 2025, 15, 4462. https://doi.org/10.3390/app15084462
17. https://www.nottingham.ac.uk/Research/Groups/Advanced-Materials-Research-Group/Images/Energy-Materials/SOFC-466.jpg
18. Current Density Distribution in Solid Oxide Fuel Cell. COMSOL Multiphysics Tutorial Guide. Available online: https://cn.comsol.com/model/current-density-distribution-in-a-solid-oxide-fuel-cell-514
19. Borgnakke C, Sonntag RE. (1997). Thermodynamic and transport properties. *(No Title)*.
20. Todd B, Young JB. Thermodynamic and transport properties of gases for use in solid oxide fuel cell modelling.2002. Journal of power Sources, 2002. 110(1), 186-200. https://doi.org/10.1016/S0378-7753(02)00277-X
21. Ranasinghe SN, Middleton PH. Modelling of single cell solid oxide fuel cells using COMSOL multiphysics. In: the proceeding of 2017 IEEE International Conference on Environment and Electrical Engineering and 2017 IEEE Industrial and Commercial Power Systems Europe. 06-09 June 2017 .Milan, Italy.
22. Hussain, MM, Baschuk JJ, Li X, et al. Thermodynamic analysis of a PEM fuel cell power system. 2005 International journal of thermal sciences; 44(9), 903-911. https://doi.org/10.1016/j.ijthermalsci.2005.02.009
23. Khazaee I, Rava A. Numerical simulation of the performance of solid oxide fuel cell with different flow channel geometries. 2017; Energy, 119, 235-244. https://doi.org/10.1016/j.energy.2016.12.074
24. Ouba AKDO, Chinelatto AL, Borcezi JS, et al. Influence of the Number of Dimensions in the Impedance Spectroscopy Simulation of a YSZ Electrolyte. Materials Research. 2022; 25, 20220259. https://doi.org/10.1590/1980-5373-MR-2022-0259
25. Iliev IK, Gizzatullin AR, Filimonova AA, et al. Numerical Simulation of Processes in an Electrochemical Cell Using COMSOL Multiphysics. Energies. 2023; 16: 7265. https://doi.org/10.3390/en16217265

26. Singhal SC, Kendal K. High temperature and solid oxide fuel cells: fundamentals, design and applications. 1st ed. USA: Elsevier Science; 2003
27. Zhang X, Wang L, Espinoza M, et al. Numerical simulation of solid oxide fuel cells comparing different electrochemical kinetics. International Journal of Energy Research, 2021; 45(9), 12980-12995. https://doi.org/10.1002/er.6628
28. Murad A, Kumar L, Harijan K, et al. Thermal Modeling and Performance Investigation of Proton Exchange Membrane (PEM) Fuel Cell. VFAST Transactions on Mathematics. 2023; 11(2):112-125. https://doi.org/10.21015/vtm.v11i2.1640
29. Liu Y, Liu J, Fu L, et al. Numerical Study on Effects of Flow Channel Length on Solid Oxide Fuel Cell-Integrated System Performances. Sustainability. 2024; 16(4):1643. https://doi.org/10.3390/su16041643
30. Ternero F, Rosa LG, Urban P, et al. Influence of the Total Porosity on the Properties of Sintered Materials—A Review. Metals. 2021; 11(5):730. https://doi.org/10.3390/met11050730
31. Barbir F. Fuel Cell Electrochemistry. In: PEM Fuel Cells (Second Edition), 2nd ed. Elsevier; 2013. 33-72.
32. Rasheed RKA, Liao Q, Caizhi Z, et al. A review on modelling of high temperature proton exchange membrane fuel cells (HT-PEMFCs). International journal of hydrogen energy, 2017; 42(5): 3142-3165. https://doi.org/10.1016/j.ijhydene.2016.10.078
33. Bandal H, Koteshwara Reddy KK, et al. Iron-based heterogeneous catalysts for oxygen evolution reaction; change in perspective from activity promoter to active catalyst. Journal of Power Sources. 2018; 395(Issue):106-127. https://doi.org/10.1016/j.jpowsour.2018.05.047
34. Paz C, Suárez E, Cabarcos A, et al. Experimental Investigation and CFD Analysis of Pressure Drop in an ORC Boiler for a WHRS Implementation. Sensors. 2022; 22(23):9437. https://doi.org/10.3390/s22239437